INTERNAL STATE VARIABLE DESCRIPTION OF DYNAMIC FRACTURE OF DUCTILE SOLIDS

PIOTR PERZYNA†

Department of Ocean Engineering, Massachusetts Institute of Technology, Cambridge, MA 02139, U.S.A.

Abstract—The paper aims at the description of ductile fracture phenomenon in dynamic processes in inelastic solids by means of internal state variable structure. Dynamical test data for aluminum and copper have been discussed. Particular attention is given to postshot photomicrographic observations of the residual porosity and on investigation of fracture mechanisms and spalling phenomenon. Spalling process has been described as a sequence of the nucleation, growth and coalescence of microvoids. Heuristic considerations of the growth and nucleation of microvoids are presented

General evolution equation for porosity parameter is postulated. This equation describes the work-hardening viscoplastic response of solid and takes also account of the interactions of microvoids. An elastic-viscoplastic model of a material with internal imperfections is proposed. Internal imperfections are generated by the nucleation, growth and coalescence of microvoids. The model describes the dynamical behavior of dissipative solids observed experimentally as well as the mechanisms of fracture. A dynamical criterion of fracture (spalling) of metals is proposed. The criterion describes the dependence of fracture phenomenon upon the evolution of the constitutive structure.

As an application of the theory the dynamic fragmentation process is considered. Prediction of fragment size is based on a very simple evolution equation assumed for the porosity parameter. The procedure of the determination of the interaction material functions has been developed.

1. INTRODUCTION

The main objective of the paper is the description of ductile fracture phenomena in dynamic processes in inelastic solids by means of internal state variable structure. The focus is primarily on the plate-impact configuration system. This is a good example of a dynamic deformation process, and has been recently performed to investigate dynamic fracture and spalling in metals. Dynamical test data for aluminum and copper have been discussed. Particular attention is given to postshot photomicrographic observations of the residual porosity and on investigation of fracture mechanisms and spalling phenomenon. Spalling process has been successfully described as a sequence of the nucleation, growth and coalescence of microvoids. Heuristic considerations of the growth and nucleation of microvoids are presented. This approach helps to investigate quasi-static approximation and equilibrium state and to examine the influence of inertial and localized thermal effects on growth of microvoids.

General evolution equation for porosity parameter is postulated. This equation describes the work-hardening viscoplastic response of solid and takes also account of the interaction of microvoids. An elastic-viscoplastic model of a material with internal imperfections is proposed. Internal imperfections are generated by the nucleation, growth and coalescence of microvoids. The model describes the dynamical behavior of dissipative solids observed experimentally as well as the mechanism of fracture. The main role in this model plays the evolution equation for the imperfection parameter interpreted as the volume fraction of microvoids (porosity). The determination of the material functions and material constants is based on available dynamical data and on metallurgical observations for copper and aluminum. A dynamical criterion of fracture (spalling) of metals is proposed. The criterion describes the dependence of fracture phenomenon upon the evolution of the

† Visiting Professor. On leave from the Institute for Fundamental Technological Research, Polish Academy of Sciences, Warsaw, Poland.

constitutive structure. This criterion is sensitive to the particular choice of the yield condition and to the evolution equation proposed for the void volume fraction parameter.

As an application of the theory the dynamic fragmentation process is considered. An approach presented by Grady[7] is utilized whereby surface or interface area created in the fragmentation process is governed by an equilibrium balance of the surface or interface energy and a local inertial or kinetic energy. Two examples are fragmentation due to ductile fracture under impact loading and fragmentation due to shear banding in shock-compression plastic deformation. Prediction of fragment size is based on a very simple evolution equation assumed for the porosity parameter. It has been proved that the criterion proposed describes dynamic fracture as a time-dependent phenomenon. This implies that the fragmentation process does depend on the stress pulse duration. Comparison of theoretical predictions with experimental observations and the discussion of the results obtained are given.

The procedure of the determination of the nucleation and growth interaction material functions in the phenomenological evolution equation for the porosity parameter has been developed.

2. EXPERIMENTAL RESULTS AND PHYSICAL FOUNDATIONS

2.1. *Discussion of experimental results*

The most popular dynamical experiment† investigating the fracture phenomenon in metals is a plate-impact configuration system. This experimental system consists of two plates, a projectile plane plate impacts against a target plane plate. This is a good example of a dynamic deformation process. If impact velocity is sufficiently high the propagation of a plastic wave through the target is generated. The reflection and interaction of waves result in a net tensile pulse in the target plate. If this stress pulse has sufficient amplitude and sufficient time duration, it will cause separation of the material and spalling process.

The reason for choosing this particular kind of dynamical experiment is that postshot photomicrographic observations of the residual porosity are available, and the stress amplitude and pulse duration can be performed sufficiently great to produce substantial porosity at the spall of the target plate.

The experimental data presented by Seaman *et al.*[25] illustrate damage phenomena and provide a common basis for considering damage criteria. They have used a plate-impact configuration system. Following the compression waves resulting from the impact, rarefaction waves have intersected near the middle of the target plate to cause damage in the form of nearly spherical voids. The heaviest damage is localized in a narrow zone, which is called the spall plane. Both the number and the size of voids decrease with distance from this zone. This type of damage is termed ductile fracture because of high ductility (ability to flow) required of the plate material.

The final damage of the target plate (aluminum 1145) for a constant shot geometry but for different impact velocities has been performed by Barbee *et al.*[1]. The results suggest dependence of spalling process on the pulse amplitude. On the other hand an example of brittle fracture in Armco iron (cf. Ref. [25]) shows dependence of damage on the tensile pulse duration. In this experimental performance an Armco iron target was impacted by a flyer plate, which was tapered on the back to provide a varying tensile wave duration across the plate. The damage, which appears as randomly oriented microcracks, varies in proportion to the tensile wave duration.

A sample of full separation is shown in Fig. 1, an aluminum target impacted by a flat plate has been damaged to the extent that full separation occurred near the center of the target, cf. Ref. [25]. The authors suggested that this full separation appears as a macrocrack propagating through heavily damaged material. The macrocrack occurs as a result of coalescence of microvoids which is visible in Fig. 1.

Similar experimental test data have been obtained for copper by Seaman *et al.*[24].‡

---

† For a thorough discussion of the experimental and theoretical works in the field of dynamic fracture and spalling of metals please consult the review paper by Meyers and Aimone[13].
‡ The experimental results of this unpublished report can be found in the recent paper by J. N. Johnson[11].

Fig. 1. A sample of full separation of an aluminum target. Impact test performed by Seaman *et al.*[25].
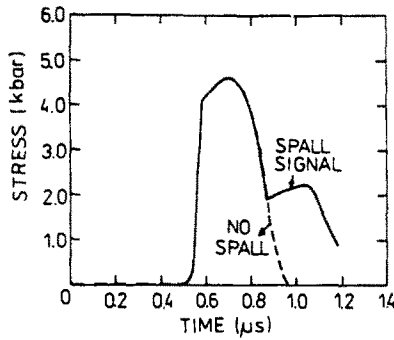
Fig. 2. The pressure gauge record for copper. A plate-impact experiment performed by Seaman *et al.*[24].

This is also a plate-impact experiment in which a 0.6 mm thick copper plate strikes a 1.6 mm copper target backed by a relatively thick plate of PMMA (polymethylmethacrylate) in which a manganin pressure gauge is embedded. The impact velocity of 0.016 cm/μs implies a 29-kbar peak tensile stress in the copper target, and pulse duration of about 0.3 μs which are sufficient to produce porosity up to 32% at the spall plane. The manganin pressure gauge record is shown in Fig. 2. The postshot photomicrographic observations of final porosity or the void volume fraction in the copper target are shown in Fig. 3.

From the experimental investigations we have the following conclusions:

1. Damage (spalling) in ductile metals (aluminum, copper, mild steel, etc.) depends on the amplitude of tensile stress as well as on the duration of stress pulse. So, to characterize dynamic fracture one has to use the stress impulse or some other stress–time integral quantity, cf. Ref. [24].

2. As the damage occurs the stiffness of the material decreases. This softening of the material is mainly due to the nucleation, growth and coalescence of microvoids (sometimes thermal effects are also pronounced).

3. Full separation (fracture, fragmentation, spalling) is the result of the coalescence of microvoids and appears as a macrocrack propagating through heavily damaged material.

4. The propagation of the shock plastic wave induced by the impact process produces significant substructural changes which affect the mechanical properties. In general, one observes an increase in the flow stress with a corresponding decrease of ductility.

2.2. *Physical mechanism of ductile dynamic fracture*

To understand better the physical mechanism of ductile dynamic fracture let us consider the variation of tensile stress with porosity or void volume fraction, cf. Fig. 4. The trajectory
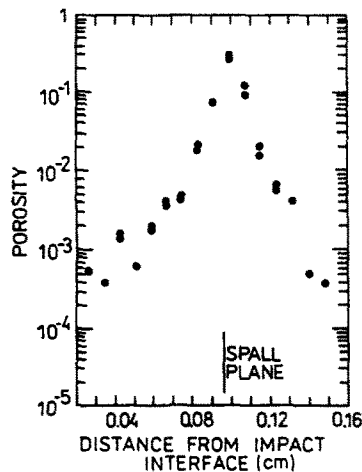

Fig. 3. The postshot photomicrographic observations of final porosity in a copper target, cf. Seaman *et al.*[24].
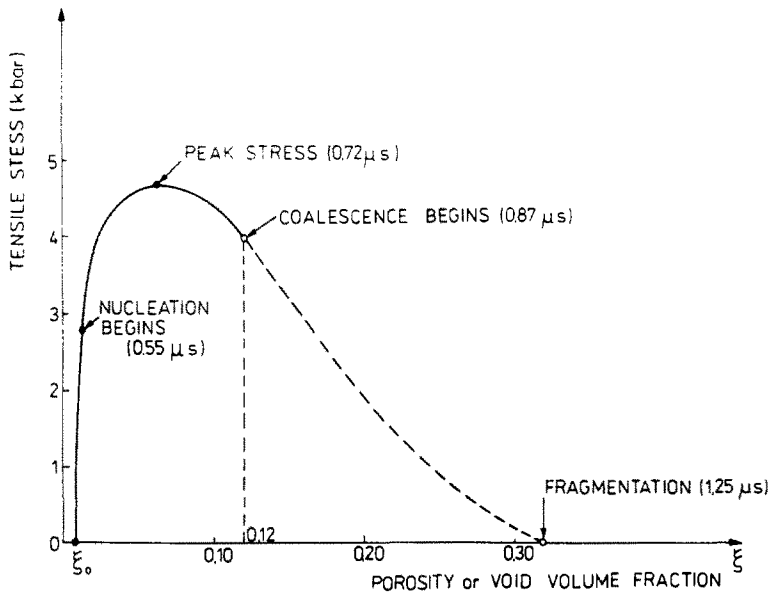
Fig. 4. Tensile stress as a function of porosity in a dynamic process for copper specimen.

tensile stress–porosity represents the real dynamic process in the copper target (specimen). The process starts at the initial porosity ζ_0 and in about 0.55 μs tensile stress reaches the point at which the nucleation of microvoids can be detected. The process goes on, tensile stress peaks up at 0.72 μs and slowly breaks down to attain in 0.87 μs the point at which the coalescence of microvoids begins. At this point the fragmentation process by the coalescence of microcracks has started. The segment of the dynamic process marked by the dashed line represents the mechanism of ductile fracture (spalling or fragmentation) which ends at zero tensile stress. The duration of the entire dynamic deformation process in the copper target (as it has been suggested by experimental observations) is approximately 1.25 μs.

From this analysis of the dynamic deformation process one can see that the main cooperative phenomena which are most important for proper description of dynamic fracture (spalling) are as follows:

1. The plastic deformation wave phenomena.
2. The nucleation and growth of microvoids.
3. The coalescence of microvoids which leads to fragmentation process.
4. Full separation as a result of the propagation of a macrocrack through heavily damaged material.

3. HEURISTIC CONSIDERATIONS FOR GROWTH AND NUCLEATION OF MICROVOIDS

3.1. Description of void growth

Carroll and Holt[2] and Johnson[11] have developed a very useful model of description of void growth in ductile materials. In the model of Carroll and Holt[2] static and dynamic pore-collapse relations for porous ductile materials have been derived. It has been done by analysis of the collapse of a hollow sphere of appropriate pore radius and over-all porosity under external pressure. It has been assumed that the matrix material is homogeneous, isotropic, incompressible and elastic-perfectly plastic.† This model however does not take into consideration the full interactions of voids.

In our heuristic considerations we shall take advantage of the model developed by

---

† Johnson[11] has generalized this development by taking account of viscosity effects. Cf. also very recent study by Freund and Hutchinson[6].

Carroll and Holt[2] and Johnson[11] and we shall apply it to the case when material of a body has work-hardening viscoplastic properties.

Carroll and Holt[2] have proved that the elastic compressibility does not significantly affect the result for elastic-perfectly plastic material.

Therefore we may introduce very useful simplification (similar as it has been assumed by Johnson[11]).

When dealing with void growth in materials of very low initial porosities, we can neglect the initial elastic and elastic-viscoplastic phases of the process and go immediately to the case of fully viscoplastic deformation around the void.

Let us consider a rectangular volume element containing a representative distribution of voids and assume a uniform hydrostatic tension $\bar{p}$ acting over the surface of this element (cf. Johnson[11]).

Since the cross-sectional area occupied by the voids supports none of this stress, mechanical equilibrium requires that

$$A_s\bar{p}_s + (A - A_s)p_g = A\bar{p}, \tag{3.1}$$

where $\bar{p}_s$ is the mean stress in the solid material which subtends an average area A_s on plane of total area A and p_g is the internal gas pressure. For a random distribution of hole shapes and sizes $(A_s/A) = (V_s/V)$ and we have that the mean stress in solid constituent is

$$\bar{p}_s = \frac{1}{1-\xi}\bar{p} - \frac{\xi}{1-\xi}p_g, \tag{3.2}$$

where

$$\xi = \frac{V - V_s}{V} \tag{3.3}$$

is the void volume fraction (or porosity).

Following Johnson[11] let us consider a single spherical void of radius a in a sphere of radius b subject to internal pressure p_g and external stress

$$\sigma_{rr} = -\frac{1}{1-\xi}\bar{p} + \frac{\xi}{1-\xi}p_g.$$

The equation of motion for material surrounding the void is as follows (in the Eulerian spherical coordinates r, θ, ϕ)

$$\rho_s\ddot{r} = \frac{\partial\sigma_{rr}}{\partial r} + 2(\sigma_{rr} - \sigma_{\theta\theta})\frac{1}{r}, \tag{3.4}$$

where ρ_s is the solid density and σ_{rr} and $\sigma_{\theta\theta}$ are the radial and circumferential deviatoric stresses.

The material of the matrix is assumed work-hardening viscoplastic. So, the second invariant of the stress deviation is related to the square root of the second invariant of the plastic strain rate $\dot{\bar{\varepsilon}}^p$ by (cf. Refs. [14–17])

$$\sqrt{J_2'} = Y\left\{1 + \Phi^{-1}\frac{\dot{\bar{\varepsilon}}^p}{\gamma_0}\right\}, \tag{3.5}$$

where

$$Y = Y_0 + H(\bar{\varepsilon}^p) \tag{3.6}$$

is the plastic strain dependent yield stress due to work-hardening effects.

We shall apply the linearized form of the relations (3.5) and (3.6), namely

$$\sigma_{\theta\theta} - \sigma_{rr} = Y_0 + H'\bar{\varepsilon}^p + \bar{\eta}\dot{\bar{\varepsilon}}^p, \tag{3.7}$$

where

$$\bar{\eta} = \frac{\hat{B}}{\rho_M \hat{b}^2} \tag{3.8}$$

and $\hat{B}$ denotes the dislocation drag coefficient, ρ_M is the mobile dislocation density and $\hat{b}$ denotes the Burgers vector.

The linearized form (3.7) of the work-hardening viscoplastic model can be treated as an approximation of nonlinear viscoplastic response obtained for the high velocity dislocation damping mechanism (cf. Ref. [16]).

Application of the model (3.7) by means of the procedure developed in Carroll and Holt[2] and Johnson[11] to the boundary value problem described by eqn (3.4) and

$$\sigma_{rr}(a, t) = -p_g \tag{3.9}$$

$$\sigma_{rr}(b, t) = -\frac{1}{1-\xi}\bar{p}(t) + \frac{\xi}{1-\xi}p_g$$

gives the evolution equation for the porosity parameter in the form as follows

$$\tau^2 Y_0[\ddot{\xi}I_1(\xi) + (\dot{\xi})^2 I_2(\xi)] + \eta\frac{\dot{\xi}}{\xi}F_2(\xi, \xi_0) = \frac{1}{1-\xi}\Delta p, \tag{3.10}$$

where τ is called the relaxation time of the inertial effects and is defined by

$$\tau^2 = \rho_s a_0^2 / 3 Y_0 \left(\frac{\xi_0}{1-\xi_0}\right)^{2/3}. \tag{3.11}$$

a_0 denotes the initial radius of the void, ξ_0 is the initial porosity, and

$$I_1(\xi) = -\frac{\xi^{-1/3} - 1}{(1-\xi)^{5/3}},$$

$$I_2(\xi) = \frac{1}{6(1-\xi)^{8/3}}[\xi^{-4/3} - 1] - \frac{2}{(1-\xi)^{8/3}}[\xi^{-1/3} - 1],$$

$$F_2(\xi, \xi_0) = \frac{2}{3(1-\xi_0)}\left(\frac{1-\xi_0}{1-\xi}\right)^{2/3}\left[\xi - \left(\frac{\xi_0}{\xi}\right)^{1/3}\right], \tag{3.12}$$

$$\Delta p = \bar{p}(t) - p_{\text{eqn}}(\xi),$$

$$\eta = \frac{2}{3}\bar{\eta},$$

where

$$p_{\text{eqn}}(\xi) = p_g \pm \frac{2Y_0}{3}(1-\xi)\ln\left(\frac{1}{\xi}\right) \mp \frac{2H'}{3}(1-\xi)F_1(\xi, \xi_0),$$

and

$$F_1(\xi, \xi_0) = 3\left(\frac{1-\xi}{1-\xi_0}\right)^{1/3}\left[1 - \left(\frac{\xi_0}{\xi}\right)^{1/3}\right]. \tag{3.13}$$

3.2. *Quasi-static approximation*

Equation (3.10) describes the microvoid growth in rate dependent work-hardening plastic material. The first term on the left hand side of eqn (3.10) gives account of inertial effects on void growth. This term depends on the relaxation time τ defined by the relation of eqn (3.11). The influence of the inertial effects on the microvoid growth process has been investigated by Johnson[11]. It seems that rate-dependent void growth is initially dominated by plastic flow rather than inertial effects but it is not a general conclusion and each case has to be investigated separately.

However, for practical purposes it would be reasonable to investigate the quasi-static approximation of the evolution equation for the porosity parameter ξ. To do this let us assume $\tau = 0$ and additionally $p_g = 0$, then eqn (3.10) gives

$$\dot{\xi} = \frac{1}{\eta} F(\xi, \xi_0)\Delta p, \tag{3.14}$$

where

$$F(\xi, \xi_0) = \frac{3}{2}\xi\left(\frac{1-\xi_0}{1-\xi}\right)^{1/3}\left[\xi - \left(\frac{\xi_0}{\xi}\right)^{1/3}\right]^{-1}. \tag{3.15}$$

The evolution eqn (3.14) is sufficiently simple to give a good basis for the phenomenological description of the void growth during a dynamical deformation process.

3.3. *Discussion of the equilibrium state*

The equilibrium state is reached when $\dot{\xi} = 0$, then the evolution eqn (3.14) yields

$$\Delta p = 0 \tag{3.16}$$

or

$$p = p_{\text{eqn}}(\xi) = \pm\frac{2Y_0}{3}(1-\xi)\ln\left(\frac{1}{\xi}\right) \mp \frac{2H'}{3}(1-\xi)F_1(\xi, \xi_0). \tag{3.17}$$

The relation of eqn (3.17) shows direct influence of work-hardening effect on the value of the equilibrium pressure $p_{\text{eqn}}(\xi)$ for particular porosity ξ. The work-hardening increases the equilibrium pressure that has been shown in Fig. 5. The work-hardening effect for porosity $\xi = \xi_1$ is described by the segment AA'. It is noteworthy that the segment AA' is decreasing function of the porosity parameter ξ. However, for practically important values of ξ, that is from the interval $[\xi_0, \xi^F]$ where ξ^F denotes the value of ξ at fracture, the work-hardening effect is pronounced.

This effect is rather large due to large plastic deformations accompanying the microvoid growth process.

In the theory developed the yield strength of the material is strain rate and plastic strain dependent. This seems reasonable because of the large amount of work-hardening that occurs in the vicinity of a growing microvoid.

3.4. *Nucleation of microvoids*

In recent years the physical foundations of the nucleation of microvoids in ductile metals is the subject of active investigations. It seems however that many aspects concerning the nucleation process are still unclear and need more research work.

The rate processes associated with microscopic flaws govern failure by ductile fracture or the formation of shear band localizations. Most structural solids (e.g. metals and alloys) contain large microscopic flaws, such as inclusions, grain boundaries, second phase particles, etc. Every solid has an inherent distribution of flaws of various sizes and orientations.

Microscopic flaws that are exposed to a combination of tensile and shear stresses will
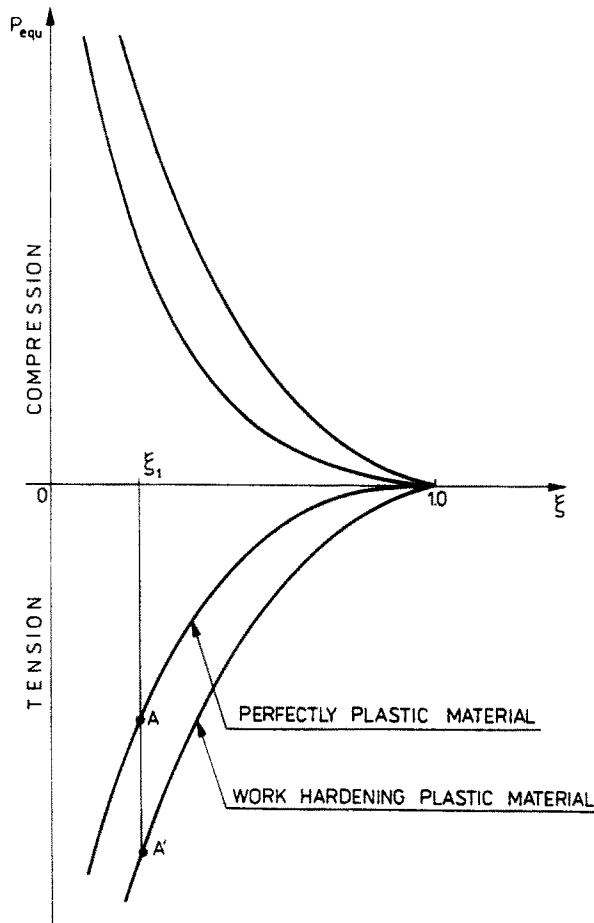
Fig. 5. The equilibrium pressure–porosity curves for perfectly plastic and work-hardening plastic
materials.

tend to become activated as opening microvoids that grow as long as the tensile stress
remains above a threshold value.

For example in steels, a large number of microvoids are found to nucleate at particle–
matrix interface. Experimental metallurgical observations suggest that microvoids are much
more likely to occur at embrittled grain boundaries and brittle second-phase particles than
as a result of twin or slip interactions. Almost every microcrack found in 0.035% C and
0.005% C steels could be traced to the fracture of a carbide particle (cf. Meyers and
Aimone[13]).

Shockey *et al.*[27] classify nucleation into two groups: homogeneous and hetero-
geneous. As homogeneous they treat microfracture nucleation at submicroscopic hetero-
geneities such as low-angle grain boundaries, dislocation tangles and networks, and fine
impurity or precipitate particles. As heterogeneous the nucleation sites are assumed to be the
ones visible by optical microscopy (at a magnification of 1000 ×).

The homogeneous nucleation is governed only by thermal fluctuation process.

The heterogeneous nucleation sites are as follows:

1. Inclusions and second-phase particles. There are three different manners in which
fracture initiation might take place:

(a) Fracture of inclusions. The brittle inclusions by breaking creates a microcrack that
operates as a stress-concentration site for the matrix.

(b) Separation of interfaces. When the particle is not strongly bounded to the matrix,
the separation produces an effective void size that has size of the particle.

(c) Fracture of the matrix. When the fracture strength of the matrix is less than that
of the inclusion or interface.

2. Fracture at grain boundaries. The presence of a weak phase at grain boundaries favors microcrack initiation there.

The authors of the paper[27] believe that both homogeneous and heterogeneous nucleation occur concurrently, if the stress is high enough. The threshold stress of heterogeneous nucleation is, of course, lower than the one for homogeneous nucleation. Most studies have concentrated on the low-to-moderate damage region and heterogeneous nucleation might be the main fracture mechanism. On the other hand, higher stresses (above the thresholds for both) will probably induce both homogeneous and heterogeneous nucleation.

Curran et al.[3, 27] have analyzed the mechanism of nucleation, growth and coalescence of microflaws for the various modes of deformation. They have proposed the following evolution equation for the number of microvoids per unit volume

$$\dot{N} = \frac{\partial N}{\partial t}\bigg|_x = A(\sigma, \theta) + B(\sigma)\dot{\sigma} + C(\bar{\varepsilon}^p)\dot{\bar{\varepsilon}}^p, \tag{3.18}$$

where $\sigma = 1/3(\sigma_{ii})$ is the hydrostatic stress, $\bar{\varepsilon}^p$ is the equivalent plastic deformation and θ denotes temperature.

The first term $A(\sigma, \theta)$ describes nucleation under constant stress as a result of a thermally-activated mechanism. This term is comparable to the proposition for the nucleation rate derived by Raj and Ashby[23]. Diffusional processes are the mode of forming the void nucleus according to this mechanism.

The second term $B(\sigma)\dot{\sigma}$ describes nucleation arising from debonding at second-phase particles as the stress progressively increases.

The third term $C(\bar{\varepsilon}^p)\dot{\bar{\varepsilon}}^p$ is introduced to describe the nucleation by debonding due to plastic strain accumulation.

For dynamical processes the thermally-activated mechanism of the nucleation of microvoids is the most important. To prove this conjecture it is sufficient to investigate the time duration needed for every nucleation mechanism considered and to compare with the time duration of the impact process itself.

So, in our description of dynamical fracture we shall use only the first term which may be approximated by

$$A(\sigma, \theta) \approx \exp\left(\frac{m|\sigma - \sigma_N|}{k\theta}\right) - 1, \tag{3.19}$$

where $m|\sigma - \sigma_N|$ is the activation energy for the nucleation mechanism, σ_N denotes the threshold stress for the nucleation, m is the material coefficient, k denotes the Boltzmann's constant and θ is actual temperature.

It is noteworthy that the assumption of eqn (3.19) is consistent with the proposition of Zhurkov[28] who treats nucleation as a statistical rate process.

3.5. Influence of thermal effects

It seems that thermal effects might have in many cases a dominant role in the mechanism of growth and nucleation of microvoids. Of course, it depends on the range of temperature changes. For instance, for elevated temperature the nucleation and growth of microvoids in metals will be governed by different mechanisms than for room temperature. The mechanisms of nucleation and growth of microvoids are very sensitive to temperature changes.

As it has been investigated by Johnson[11] even for room temperature in surroundings of a body considered for heterogeneous plastic deformation there exists substantial localized heating effects. Plastic shear strains of several thousand percent are developed at the expanding pore walls. The magnitude of the corresponding temperature change estimated by calculating the plastic shear strain at the pore wall is a substantial fraction of the melting temperature of a material.

These localized thermal effects can influence the growth mechanism by softening of the strength of a material as well as the nucleation mechanism by changing rate of the thermally-activated process.

4. PHENOMENOLOGICAL DESCRIPTION OF THE NUCLEATION, GROWTH AND COALESCENCE OF MICROVOIDS

4.1. *Interaction of microvoids*

The generation and propagation of spall fracture under dynamic loading are only partially understood metallurgically. The complexity of the situation can be assessed by careful investigation of possible fracture mechanism.

There are essentially two modes of dynamic fracturing: brittle and ductile. Brittle fracture is characterized by microcracks with sharp tips at which fracture proceeds with relatively little plastic deformation. Ductile fracture, on the other hand, is characterized by microvoids which in spalling tend to be spherical up to a certain size. This mode of fracture progresses mainly due to the growth and coalescence mechanisms. Both these mechanisms are accompanied with localized large plastic deformations and very serious mutual interactions of microvoids.

BCC and HCP metals tend to spall by brittle mode, whereas FCC metals exhibit a higher ductility at large strain rates and tend to spall in a ductile manner.

For phenomenological description of ductile fracture under dynamic loading the interaction of microvoids is one of the most important effects. There are several reasons for that.

First, every microvoid is a source of singularity in the distribution of stress field in a body.

Second, the mutual interactions of microvoids can seriously influence the growth mechanism.

Third, when the deformation process is advanced then the growth mechanism and the mutual interactions of microvoids cause the coalescence phenomenon which leads directly to ductile fracture.

Fourth, as a result of interaction we can expect very important change of the threshold stress for nucleation as well as for growth mechanisms.

4.2. *General evolution equation for the porosity parameter ξ*

It is intended to base the phenomenological description of the nucleation, growth and coalescence of microvoids on heuristic considerations. We would also like to take account of the full interactions of microvoids and to treat the microvoid growth process in quasi-static approximation.

It has been postulated that internal imperfections in solids are generated by the nucleation and growth of microvoids. So, the evolution equation for the imperfection parameter ξ can be assumed in the form as follows

$$\dot{\xi} = (\dot{\xi})_{\text{nucleation}} + (\dot{\xi})_{\text{growth}}. \tag{4.1}$$

Physical considerations in Section 3.4 have shown that the nucleation of microvoids in impact processes which are characterized by very short time duration is governed by the thermally-activated mechanism.

Based on this heuristic suggestion we postulate

$$(\dot{\xi})_{\text{nucleation}} = \frac{h(\xi)}{1-\xi}\left[\exp\left(\frac{m|\sigma - \sigma_N|}{k\theta}\right) - 1\right], \tag{4.2}$$

where $h(\xi)$ is the nucleation material function which describes the effects of interactions of microvoids and the coefficient $(1-\xi)^{-1}$ is introduced to describe singularity observed experimentally.†

† For experimental justification of this assumption, see Garber *et al.*[8].

For the growth process we postulate [cf. eqn (3.14)]

$$(\dot{\xi})_{\text{growth}} = \frac{g(\xi)}{\eta} F(\xi, \xi_0) \Delta\sigma, \tag{4.3}$$

where $F(\xi, \xi_0)$ is given by eqn (3.15), $\Delta\sigma = \sigma - \sigma_G$, and the threshold stress for the growth σ_G is proportional to the growth equilibrium stress

$$\sigma_G = k_1 \left[\frac{2}{3} Y_0(1-\xi) \ln\left(\frac{1}{\xi}\right) - \frac{2H'}{3}(1-\xi)F_1(\xi, \xi_0) \right], \tag{4.4}$$

where k_1 is the interaction coefficient and $g(\xi)$ is the growth material function which describes the effects of the interactions of microvoids.

As a result of these assumptions we have the evolution equation for the void volume fraction parameter ξ in the form

$$\dot{\xi} = \frac{h(\xi)}{1-\xi} \left[\exp\left(\frac{m|\sigma - \sigma_N|}{k\theta}\right) - 1 \right] + \frac{g(\xi)}{\eta} F(\xi, \xi_0)\Delta\sigma. \tag{4.5}$$

The crucial point in the phenomenological description is the determination of the nucleation and growth material functions. Both functions h and g have been introduced to describe mutual interaction effects for microvoids. The procedure of the determination of the material functions h and g has to be based on the global results of fracture during dynamical processes of considered solid. We shall discuss this problem in Section 6.

5. ELASTIC-VISCOPLASTIC MODEL OF VOIDED SOLID

5.1. Constitutive and evolution equations

Impact processes are characterized by very short time duration and by very large strain rates. The time duration is of the order of 1.25–1.50 μs and the strain rate can attain values 10^4–10^6 s^{-1}. To describe such processes it is important to take into consideration time dependency or strain rate sensitivity of a material. This can be achieved within the framework of viscoplasticity theory.

There is no need to point out the advantages that can be gained by simultaneous description of rheological and plastic effects. As a result of simultaneous introduction of viscous and plastic properties, we obtain a dependence on the load history and on time. A description of deformation in viscoplasticity will therefore involve the history of the specimen, expressed in the type of loading process, and the time duration. Different results will be obtained for different loading paths and different durations of the process.†

In the previous papers[18–21] of the author a simple model of an elastic-viscoplastic solid with internal imperfections has been proposed. The model has been developed within the framework of the internal state variable structure. The model proposed has been applied to the description of quasi-static plastic flow processes.

In the present paper we shall propose the alternative model of an elastic-viscoplastic voided solid with the aim of application to the description of dynamic fracture in impact processes.

For dynamic processes not only viscoplastic properties but also elastic properties of a material depend on the porosity parameter ξ. So, the shear and bulk moduli are assumed to be degraded by the presence of microvoids according to a model suggested by

† These features are very important in the description of fracture phenomenon, which depends on the amplitude of loading as well as time duration.

MacKenzie[12] (cf. also Johnson[11])

$$\bar{G} = G_0(1-\xi)\left(1 - \frac{6K_0+12G_0}{9K_0+8G_0}\xi\right)$$

$$\bar{K} = 4G_0K_0(1-\xi)/(4G_0+3K_0\xi),$$

(5.1)

where G_0 and K_0 are the elastic moduli of unvoided material.

As a result the Poisson ratio $\bar{v}$ is determined by the relation

$$\bar{v} = \frac{1}{2}\frac{3\bar{K}-2\bar{G}}{3\bar{K}+2\bar{G}}.$$

(5.2)

Let us denote the symmetric rate of deformation tensor by **D** and postulate†

$$\mathbf{D}^e = \mathbf{D} - \mathbf{D}^p$$

$$\mathbf{D}^e = \frac{1}{2\bar{G}}\left[\overset{\triangledown}{\sigma} - \frac{\bar{v}}{1+\bar{v}}\operatorname{tr}\overset{\triangledown}{\sigma}\mathbf{I}\right]$$

(5.3)

$$\mathbf{D}^p = \frac{\gamma_0}{\psi}\left\langle\Phi\left[\frac{f(\cdot)}{\kappa}-1\right]\right\rangle\partial_\sigma f$$

where $\overset{\triangledown}{\sigma}$ denotes the symmetric Zaremba–Jaumann rate of change of the Cauchy stress tensor σ, **I** denotes the unit tensory, γ_0 is the viscosity constant, ψ is introduced as the control function and is assumed to depend on $(I_2/I_2^s)-1$, where I_2 is the second invariant of the rate of the deformation tensor and I_2^s is its static value, Φ denotes the viscoplastic overstress function, f is the quasi-static yield function which is postulated to depend on the first invariant of the Cauchy stress tensor J_1, on the second and third invariants of the stress deviator J_2' and J_3' and on the imperfection internal state variable ξ interpreted as the void volume fraction (or porosity) parameter, $\kappa = \hat{\kappa}(\bar{\varepsilon}^p, \xi)$ is the material work-hardening-softening function, the symbol $\langle[\ ]\rangle$ is understood according to the definition

$$\langle[\ ]\rangle = \begin{cases} 0 & \text{if } f \leqslant \hat{\kappa}(\bar{\varepsilon}^p,\xi) \\ [\ ] & \text{if } f > \hat{\kappa}(\bar{\varepsilon}^p,\xi). \end{cases}$$

(5.4)

We postulate the particular form of the yield function

$$f(\cdot) = J_2'\left(1 + n\xi\frac{J_1^2}{J_2'}\right),$$

(5.5)

where n denotes the material constant, and the work-hardening-softening material function

$$\kappa = \hat{\kappa}(\bar{\varepsilon}^p,\xi) = (\kappa_0 + H'\bar{\varepsilon}^p)^2(1 - n_4\xi^{1/2})^2,$$

(5.6)

where $\kappa_0 = Y_0$ denotes the yield stress, H' is the work-hardening coefficient and n_4 is the material constant.

For simplicity we assume

$$\Phi = \left[\frac{f(\cdot)}{\kappa}-1\right]^m, \quad \text{with } m = 1.$$

(5.7)

This assumption has clear physical meaning. It gives description of the rate sensitive plastic material when the dissipative mechanism is governed by the phonon viscosity

---

†The evolution equation of the modified theory of viscoplasticity in the form of eqn (5.3) has been first introduced in Ref. [17]. The physical foundations of the modified theory of viscoplasticity and identification procedure of the material functions and constants in the case of advanced strains have been presented in Ref. [22].

resistance to the dislocation motion, which takes place for very large strain rates, cf. Ref. [16].

It is also consistent with the previously introduced approximation for heuristic considerations of the growth of microvoids.

As a result of the postulated assumptions we have

$$\mathbf{D}^p = \frac{\gamma_0}{\psi} \left\langle \frac{J'_2\left(1+n\xi\frac{J_1^2}{J'_2}\right)}{(\kappa_0+H'\bar{\varepsilon}^p)^2(1-n_4\xi^{1/2})^2} - 1 \right\rangle \frac{1}{\kappa_0}(2n\xi J_1\mathbf{I}+\mathbf{S}). \tag{5.8}$$

It is noteworthy that the evolution eqn (5.8) describes inherently the dilatational effects† generated by the nucleation, growth and coalescence of microvoids. To prove this, it is sufficient to compute

$$\mathrm{tr}\,\mathbf{D}^p = \frac{\gamma_0}{\psi} \left\langle \frac{J'_2\left(1+n\xi\frac{J_1^2}{J'_2}\right)}{(\kappa_0+H'\bar{\varepsilon}^p)^2(1-n_4\xi^{1/2})^2} - 1 \right\rangle \frac{n\xi J_1}{\kappa_0}. \tag{5.9}$$

Equations (5.3) and (5.8) lead to the evolution equation for the stress tensor σ in the form as follows:

$$\frac{1}{2\bar{G}}\left[\overset{\triangledown}{\sigma} - \frac{\bar{v}}{1+\bar{v}}\,\mathrm{tr}\,\overset{\triangledown}{\sigma}\mathbf{I}\right] = \mathbf{D} - \frac{\gamma_0}{\psi} \left\langle \frac{J'_2\left(1+n\xi\frac{J_1^2}{J'_2}\right)}{(\kappa_0+H'\bar{\varepsilon}^p)^2(1-n_4\xi^{1/2})^2} - 1 \right\rangle \frac{1}{\kappa_0}(2n\xi J_1\mathbf{I}+\mathbf{S}) \tag{5.10}$$

Equation (5.10) is the first fundamental equation describing an elastic-viscoplastic model of voided solid within the rate type theory with internal state variables.

The second fundamental equation is the evolution equation for the internal state variable ξ which is postulated in the form given by eqn (4.5).

The constitutive structure described by the evolution equations (5.10) and (4.5) is sufficiently simple in its nature so that it can be applicable to the solution of the initial-boundary-value problems.

5.2. Phenomenon of dynamic fracture

As it has been discussed in Section 2 the dynamic ductile fracture is a result of two cooperative phenomena, namely the inelastic deformation process and the micro-damage process generated by the nucleation, growth and coalescence of microvoids.

From Fig. 4 one can see that during a real dynamic flow process the porosity parameter can change from $\xi = \xi_0$ to $\xi = \xi^s$, where ξ^s is called the fracture (or spalling) porosity, i.e. $\xi \in [\xi_0, \xi^s]$.

The segment of the trajectory in Fig. 8 for $\xi \in [\xi^c, \xi^s]$ (for copper $\xi^c = 0.12$ and $\xi^s = 0.32$) represents the description of dynamic ductile fracture mechanism, where ξ^c is defined as a value of porosity at which the coalescence of microvoids begins. During the segment of the flow process which corresponds to the interval $[\xi^c, \xi^s]$ the coalescence of microvoids plays the most important role and at the end of this segment when $\xi = \xi^s$ the full fragmentation (spalling phenomenon) takes place.

It is understood that for $\xi = \xi^s$ catastrophe takes place, that is

$$\kappa = \hat{\kappa}(\bar{\varepsilon}^p, \xi)|_{\xi=\xi^s} = 0, \tag{5.11}$$

then the material loses its stress carrying capacity. At $\xi = \xi^s$ one can observe full separation of the material (cf. Fig. 5).

---

† Different conception of the description of the dilatational effects in an elastic-viscoplastic damaged solid has been proposed by Davison et al.[4] and Davison and Kipp[5].

5.3. *Criterion of dynamic ductile fracture (spalling)*

During dynamic inelastic flow phenomenon it is very difficult to control plastic deformation for different stages of the process considered. So it is natural to base a criterion of dynamic fracture on the control of the porosity parameter ξ.

Criterion of dynamic fracture: During the dynamic inelastic flow process the fracture phenomenon (spalling) occurs when

$$\xi = \xi^s \rightarrow \bar{\varepsilon}^p = \bar{\varepsilon}^p_F(\mathbf{D}^p, \theta) \tag{5.12}$$

which leads to the condition

$$\kappa = \hat{\kappa}(\bar{\varepsilon}^p, \xi)\Big|_{\substack{\xi = \xi^s \\ \bar{\varepsilon}^p = \bar{\varepsilon}^p_F}} = 0. \tag{5.13}$$

It is noteworthy that the condition of eqn (5.13) is equivalent to eqn (5.11) but it expresses that both critical values $\xi = \xi^s$ and $\bar{\varepsilon}^p = \bar{\varepsilon}^p_F$ influence the dynamic fracture phenomenon.

As a result of the criterion of eqn (5.12) the condition of eqn (5.13) shows that catastrophe does depend on the rate of deformation as well as on temperature.

The condition of eqn (5.13) leads directly to the particular relation

$$\hat{\kappa}(\bar{\varepsilon}^p, \xi)\Big|_{\substack{\xi = \xi^s \\ \bar{\varepsilon}^p = \bar{\varepsilon}^p_F}} = (\kappa_0 + H'\bar{\varepsilon}^p_F)^2(1 - n_4\xi^{s^{1/2}})^2 = 0, \tag{5.14}$$

hence we obtain the material constant

$$n_4 = (\xi^s)^{-1/2} \tag{5.15}$$

which is crucial for the description of the fracture phenomenon.

5.4. *Determination of the material constants*

To make particular determination of the material constants let us consider, for instance, copper. From metallurgical observation results we know that $\xi^c = 0.12$ and $\xi^s = 0.32$ (cf. Fig. 4).

The relation of eqn (5.15) gives $n_4 = 1.7677$.

For $\psi = 0$ we have the quasi-static yield criterion in the form as follows

$$J_2 + n\xi J_1^2 = (\kappa_0 + H'\bar{\varepsilon}^p)^2(1 - n_4\xi^{1/2})^2. \tag{5.16}$$

For $H' = 0$ from eqn (5.16) we have the relation

$$n = \frac{(1 - n_4\xi^{1/2})^2 - J'_2/\kappa_0^2}{\xi(J_1/\kappa_0)^2} . \tag{5.17}$$

The material constant n can be determined based on the comparison of the present proposition with the solution for copper utilizing the Gurson[9] conception.

The solution for $\xi = 0.02$ at $J'_2 = 0$ gives

$$J_1/\kappa_0 = 4.31. \tag{5.18}$$

Inserting these results into eqn (5.17) yields

$$n = \frac{[1 - 1.7677(0.02)^{1/2}]^2}{0.02(4.31)^2} = 1.5141.$$

6. APPLICATION TO DYNAMIC FRAGMENTATION PROCESS

6.1. *Global description of dynamic fragmentation*

As an application of the theory proposed the dynamic fragmentation process is considered.

One consequence of intense impulsive loading of a solid can be the fragmentation of the body into discrete parts. This may include, for example, the fragmentation process due to ductile fracture under impact loading or fragmentation due to shear banding in plastic shock-wave deformation.

An approach in global description of the dynamic fragmentation process of a solid body has been recently developed by Grady[7].

A conception presented by Grady[7] is utilized whereby surface or interface area created in the fragmentation process is governed by an equilibrium balance of the surface or interface energy and a local inertial or kinetic energy.

Grady[7] has observed that in a decomposition of the kinetic energy, the center-of-mass kinetic energy of the fragments must be conserved during fragmentation and only the kinetic energy relative to the center of mass is available to fuel the breakage process. The latter is regarded as a local kinetic energy which is available for fragmentation without violating local momentum conservation.

The total energy density is given by

$$E(A) = \frac{3\dot{\rho}}{10\rho A^2} + \gamma A. \tag{6.1}$$

The first term on the right hand side represents the local kinetic energy density, where ρ denotes the density, $\dot{\rho}$ density rate and A is the fragment surface area to volumetric ratio. The second term describes the fragment surface energy density if γ denotes the surface energy at the appropriate temperature θ.

Grady[7] has introduced a hypothesis that during the fragmentation process the forces seek to minimize the energy with respect to the fracture surface area. So at equilibrium

$$\frac{\mathrm{d}E}{\mathrm{d}A} = 0 \tag{6.2}$$

which leads to the relation

$$A = \left(\frac{3\dot{\rho}}{5\rho\gamma}\right)^{1/3}. \tag{6.3}$$

If we assume spherical fragments of equal size, then the fragment diameter is given by

$$d = 6/A. \tag{6.4}$$

6.2. *Ductile fracture mode*

Let us consider the dynamic ductile fracture in an elastic-viscoplastic voided solid. Then the density of voided solid is given by

$$\rho = \rho_s(1 - \xi), \tag{6.5}$$

where ρ_s denotes the density of an unvoided material.

The density rate is

$$\dot{\rho} = -\rho_s\dot{\xi}. \tag{6.6}$$

Equations (6.1) to (6.6) gives the result

$$d = \left[\frac{3\rho_s \xi^2}{5(1-\xi)\gamma}\right]^{-1/3}.\tag{6.7}$$

The known quantity in a steady-wave-shock-compression process is the total energy dissipated $\mathscr{E}$.†

If we assume approximately (after Grady[7])

$$\gamma = \mathscr{E}d,\tag{6.8}$$

then

$$d = \left[\frac{10(1-\xi)\mathscr{E}}{\rho_s \xi^2}\right]^{1/2}.\tag{6.9}$$

Let us assume the initial porosity $\xi = \xi_0$ and consider only the growth process. So the evolution equation for the porosity parameter ξ has the form as follows [cf. eqn (4.5)]

$$\dot{\xi} = \frac{g(\xi)}{\eta} F(\xi, \xi_0)\Delta\sigma.\tag{6.10}$$

The nominal fragment diameter is given by the relation

$$d = \frac{6\eta}{g(\xi)F(\xi, \xi_0)\Delta\sigma}\left[\frac{10(1-\xi)\mathscr{E}}{\rho_s}\right]^{1/2}.\tag{6.11}$$

6.3. Shear band localization fracture mode

It is a well known fact that shear banding not only governs the deformation response of materials but may also strongly influence the fracture behavior.

Let us consider the shear band localization fracture mode in an elastic-viscoplastic voided solid.

Accounting for the different geometry we have the mean spacing of shear bands

$$d = \frac{6\eta}{g(\xi)F(\xi, \xi_0)\Delta\sigma}\left[\frac{3(1-\xi)\mathscr{E}}{\rho_s}\right]^{1/2}.\tag{6.12}$$

6.4. Discussion of the time duration influence

To prove that both results of eqns (6.11) and (6.12) depend strongly on time duration of the tension stress impulse it is sufficient to show that the porosity ξ is the time duration dependent quantity.

To do this let us consider the evolution of eqn (6.10). We have

$$\frac{d\xi}{dt} = \frac{g(\xi)}{\eta} F(\xi, \xi_0)[\sigma(t) - \sigma_G(\xi)],\tag{6.13}$$

with $\xi(0) = \xi_0$, where the threshold stress for the growth $\sigma_G(\xi)$ is given by the relation of eqn (4.4).

For simplicity we can assume

$$\bar{\sigma}_G = \overline{\sigma_G(\xi)}\Big|_{\xi \in [\xi_0, \xi']},\tag{6.14}$$

i.e. the mean value $\bar{\sigma}_G = $ const for the growth threshold stress $\sigma_G(\xi)$.

---

†There exists a well-known method which determined the total energy dissipated in the shock-wave phenomena. The method is based on the computation of the area between the Rayleigh line and the Hugoniot curve.

Then the evolution of eqn (6.13) can be written in the form

$$\frac{d\xi}{g(\xi)F(\xi,\xi_0)} = \frac{1}{\eta}[\sigma(t) - \bar{\sigma}_G]\, dt \tag{6.15}$$

which after integration yields

$$\int_{\xi_0}^{\xi} \frac{d\zeta}{g(\zeta)F(\zeta,\xi_0)} = \frac{1}{\eta}\int_0^t [\sigma(z) - \bar{\sigma}_G]\, dz. \tag{6.16}$$

Let us introduce the denotation

$$\bar{f}(\xi,\xi_0) = \int_{\xi_0}^{\xi} \frac{d\zeta}{g(\zeta)F(\zeta,\xi_0)}, \tag{6.17}$$

then we have

$$\bar{f}(\xi,\xi_0) = \frac{1}{\eta}\int_0^t [\sigma(z) - \bar{\sigma}_G]\, dz, \tag{6.18}$$

hence we can write

$$\xi = \hat{f}\left(\xi_0, \frac{1}{\eta}\int_0^t [\sigma(z) - \bar{\sigma}_G]\, dz\right) \tag{6.19}$$

where $\hat{f}$ is a new function of the initial porosity ξ_0 and the over equilibrium stress impulse divided by the viscosity coefficient η.

The result of eqn (6.19) shows that the porosity parameter is the time duration dependent quantity.

It is noteworthy that this feature is an inherent property of an elastic-viscoplastic model of voided solid.

6.5. Comparison of theoretical predictions with experimental observations

The numerical computations are obtained for aluminum. The shock–compression impact process is considered. It is assumed

$$\sigma = 10\, GP_a$$

$$\sigma_G = \tfrac{2}{3}\kappa_0(1-\xi)\ln\left(\frac{1}{\xi}\right), \quad k_1 = 1, \quad H' = 0$$

$$\xi_0 = 0.001$$

$$\mathscr{E} = 0.4 \times 10^8\ \text{J/m}^3$$

$$\eta = \tfrac{2}{3}\, 1.5237 \times 10^4\ \text{dyn s cm}^{-3}$$

$$\kappa_0 = 4 \times 10^7\ \text{N/m}^2$$

$$\rho_s = 2.7 \times 10^3\ \text{kg/m}^3, \quad g = 1.$$

The results for the fragment size and the mean spacing of shear bands vs the porosity parameter are plotted in Fig. 6.

One can observe that both fracture modes give reasonable results for the nominal fragment diameter. It is sufficient to compare the results obtained with the experimental observations for aluminum shown in Fig. 1.
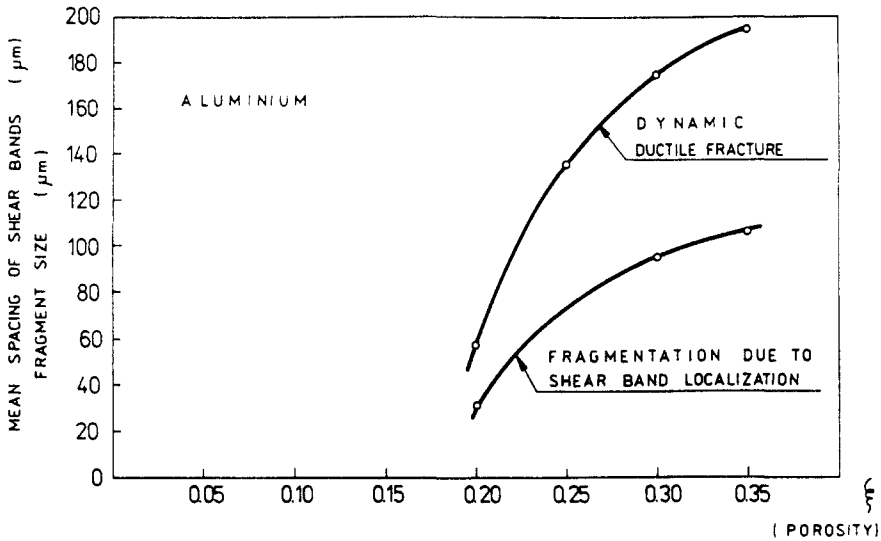
Fig. 6. The fragment size and the mean spacing of shear bands versus the porosity parameter.

Both fracture modes predict the fragmentation process only for reasonable values of the porosity parameter ξ, namely for ξ from the internal [0.18, 0.35].

It is noteworthy that the numerical computations have been performed for the growth interaction material function $g(\xi) = 1$. It seems that the results for the nominal fragment diameter can be improved for properly determining the growth interaction material function $g = g(\xi)$.

We introduce a hypothesis that the growth interaction material function g has to be determined in such a way to obtain the full saturation effect for both modes of fracture for the values of the porosity parameter ξ larger than 0.30.

The results of the performance of this proposition have been shown in Fig. 7. The results are promising and have great practical value. The procedure proposed proved that by proper determination of the growth interaction material function the results for the mean diameter of the fragment can be improved.
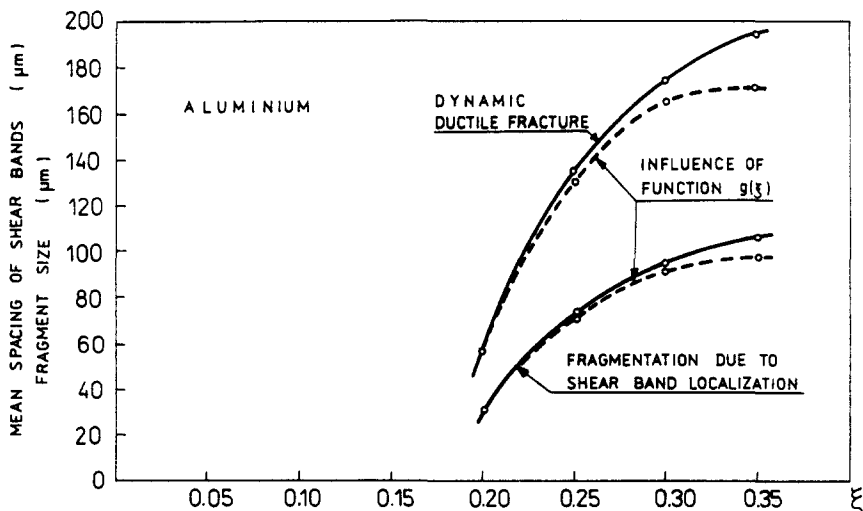

Fig. 7. Influence of the function $g(\xi)$ on the results for the fragment size and the mean spacing of shear bands vs the porosity parameter.

7. FINAL COMMENTS

The paper has brought the theory of dynamic fracture developed within the framework of the rate type constitutive structure with internal state variables. A model of an elastic-viscoplastic voided solid proposed is sufficiently simple to be applicable in the solution of initial-boundary-value problems.

It seems that the important result of the paper is a new evolution equation for the porosity parameter. This evolution equation is justified by the heuristic physical considerations and is motivated by metallurgical experimental observations.

Several effects which can influence the dynamic ductile fracture have been carefully discussed.

A criterion of dynamic ductile fracture is proposed. This criterion is inherently time dependent and it describes fracture as a final stage of the entire inelastic flow process, so that the evolution of the constitutive structure of a material is taken into consideration.

The application of the theory proposed to the dynamic fragmentation process has proved not only its usefulness but also has shown a new possibility of the determination of the growth and nucleation interaction material functions. The determination of the material functions which describe the mutual interactions of microvoids has been performed for aluminum. The results obtained have great practical value and can be used for further study of the phenomenological description of the mutual interactions of microvoids.

REFERENCES

1. T. W. Barbee, L. Seaman, R. Crewdson and D. Curran, Dynamic fracture criteria for ductile and brittle metals. *J. Mater.* **7**, 393–401 (1972).
2. M. Carroll and A. C. Holt, Static and dynamic pore-collapse relations for ductile porous materials. *J. Appl. Phys.* **43**, 1626–1636 (1972).
3. D. R. Curran, L. Seaman and D. A. Shockey, Dynamic failure in solids. *Physics Today*, pp. 46–55, January (1977).
4. L. Davison, A. L. Stevens and M. E. Kipp, Theory of spall damage accumulation in ductile metals. *J. Mech. Phys. Solids* **25**, 11–28 (1977).
5. L. Davison and M. E. Kipp, Calculation of spall damage accumulation in ductile metals, *Proc. IUTAM Symposium*, Tokyo, Japan, 1977; *High Velocity Deformation of Solids* (Edited by K. Kawata and J. Shiori), pp. 163–175. Springer, New York (1978).
6. L. B. Freund and J. W. Hutchinson, High strain-rate crack growth in rate-dependent plastic solids. Harvard University Report, June (1984).
7. D. E. Grady, Local inertial effects in dynamic fragmentation. *J. Appl. Phys.* **53**, 322–325 (1982).
8. R. Garber, I. M. Bernstein and A. W. Thompson, Hydrogen assisted ductile fracture of spheroidized carbon steels. *Metall. Trans.* **12A**, 225–234 (1981).
9. A. L. Gurson, Continuum theory of ductile rupture by void nucleation and growth. *ASME J. Engng Mater. Technol.* **99**, 2–15 (1977).
10. G. R. Irwin, Fracture, *Encyclopaedia of Physics* (Edited by S. Flugge), Vol. VI, pp. 551–591. *Elasticity and Plasticity*. Springer, New York (1958).
11. J. N. Johnson, Dynamic fracture and spallation in ductile solids. *J. Appl. Phys.* **52**, 2812–2825 (1981).
12. J. K. MacKenzie, The elastic constants of a solid containing spherical holes. *Proc. Phys. Soc.* **63B**, 2–11 (1959).
13. M. A. Meyers and C. T. Aimone, Dynamic fracture (spalling) of metals. *Prog. Mater. Sci.* **28**, 1–96 (1983).
14. P. Perzyna, The constitutive equations for rate sensitive plastic materials. *Q. Appl. Math.* **20**, 321–332 (1963).
15. P. Perzyna, Fundamental problems in viscoplasticity, *Adv. Appl. Mech.* **9**, 243–377 (1966).
16. P. Perzyna, Coupling of dissipative mechanisms of viscoplastic flow. *Arch. Mech.* **29**, 607–624 (1977).
17. P. Perzyna, Modified theory of viscoplasticity. Application to advanced flow and instability phenomena. *Arch. Mech.* **32**, 403–420 (1980).
18. P. Perzyna, Stability of flow processes for dissipative solids with internal imperfections. *ZAMP* **35**, 848–867 (1984).
19. P. Perzyna, Constitutive modelling of dissipative solids for postcritical behaviour and fracture. *ASME J. Engng Mater. Technol.* **106**, 410–419 (1984).
20. P. Perzyna, On constitutive modelling of dissipative solids for plastic flow, instability and fracture, Int. Symp. Udine, June 1983; *Proc. Plasticity Today*; *Modelling, Methods and Applications*, pp. 657–679. Elsevier, Amsterdam (1984).
21. P. Perzyna, Dependence of fracture phenomena upon the evolution of constitutive structure of solids. *Arch. Mech.* **37**, 485–501 (1985).
22. P. Perzyna and R. B. Pecherski, Modified theory of viscoplasticity. Physical foundations and identification of material functions for advanced strains. *Arch. Mech.* **35**, 423–436 (1983).
23. R. Raj and M. F. Ashby, Intergranular fracture at elevated temperature. *Acta Metall.* **23**, 653–666 (1975).

24. L. Seaman, T. W. Barbee and D. R. Curran, Stanford Res. Inst. Tech. Rep., No. AFWL-TR-71-156, Dec. (1971).
25. L. Seaman, D. R. Curran and D. A. Shockey, Computational models for ductile and brittle fracture. *J. Appl. Phys.* **47**, 4814–4826 (1976).
26. D. A. Shockey, D. R. Curran and L. Seaman, Computer modelling of microscopic failure processes under dynamic loads. *Proc. IUTAM Symposium*, Tokyo, Japan 1977, *High Velocity Deformation of Solids* (Edited by K. Kawata and J. Shiori), pp. 149–161. Springer, New York (1978).
27. D. A. Shockey, D. R. Curran and L. Seaman, *Shock Waves and High-strain Rate Phenomena in Metals: Concepts and Application* (Edited by M. A. Meyers and L. E. Murr), p. 129. Plenum Press, New York (1981).
28. S. N. Zhurkov, *Int. J. Fract. Mech.* **1**, 311 (1965).